Surface phase diagram of the Ising model with modified surface-bulk coupling

T. Lahcini and N. Benayad

Groupe de Mécanique Statistique, Laboratoire de Physique Théorique, Faculté des Sciences, Université Hassan II-Aïn Chock, B.P. 5366 Maarif, Casablanca 20100, Morocco

The phase diagram of the three-dimensional Ising system with intrasurface J_S and surface-bulk $J_\perp$ interactions modified with respect to the bulk exchange interaction J_B is studied by the use of an effective field method within the framework of a single-site cluster theory. In this investigation, the new parameter $J_\perp$ strongly affects the phase diagram obtained recently in the case $J_\perp = J_B$. Indeed, our calculations reveal some qualitatively interesting features for the surface when the bulk is ordered or disordered. Surface magnetisations are also investigated for different values of the ratio $R=J_S/J_B$..

PACS: 75.10.Hk; 75.50.Ee; 75.70.Rf

Keywords: Surface magnetism; Surface phase diagram; Surface-bulk coupling; Effective field theory

I. Introduction

During the last decades, surface magnetism has been received much attention from the theoretical and experimental points of view [1-3]. One of the simplest three-dimensional semi-infinite models is the spin-1/2 simple cubic Ising ferromagnet including two exchange interactions J_S and J_B at the surface and in the bulk, respectively. Mean-field theory [4,5], the cluster variation method [6], effective field theory [7], the finite cluster approximation [8,9], renormalization group methods [9-13], Monte Carlo techniques [14,15] and series expansions [16] predict an enriched phase diagram. Indeed, it exhibits four different types of phase transitions associated with the surface. If the ratio $R = J_S / J_B$ is greater than a critical value R_C, the system may order on the surface at a temperature higher than the bulk, followed by the ordering of the bulk at the bulk transition temperature. These two successive transitions are called the surface and extraordinary transitions, respectively. If R is less than R_C, the system orders at the bulk transition temperature. This is the ordinary phase transition. If $R = R_C$, the system orders at the bulk transition temperature but in this case the critical exponents differ from those of the ordinary transition. This is the special phase transition.

The simple cubic Ising ferromagnet with a ferromagnetic exchange interaction $(J_B > 0)$ in the bulk and an antiferromagnetic exchange interaction $(J_S < 0)$ between surface spins has also been studied using the mean-field approximation [16], the renormalization group method [17], and Monte Carlo simulation [18,19]. In this case the surface layer behaves roughly like an Ising antiferromagnet in a (temperature-dependent) field. Below the bulk critical temperature, the bulk is ordered ferromagnetically for all J_S. For a surface exchange interaction greater than some temperature-dependent value of J_S, the surface is also in an ordered ferromagnetic state, but for more negative values of J_S the surface is antiferromagnetic instead. As the temperature increases, the bulk disorders, but for strongly negative J_S the surface remains ordered up to some higher temperature. The phase boundaries for the bulk and the surface transitions cross at a tetracritical point.

In this paper, we investigate the surface phase transitions in the semi-infinite simple cubic Ising ferromagnet with an antiferromagnetic surface and a modified surface-bulk coupling $J_\perp$. The introduction of this later exchange interaction (which describe a more realistic situation) gives access to the 2D limit of the free surface realized for $J_\perp \to 0$. The aim of this work is to describe the phase diagrams of the system, by the use of an effective-field method within the framework of a single-site cluster theory. In particular, we focus our attention on the effects of the surface-bulk coupling on the phase transitions associated with the surface. The paper is organized as follows. In section 2, we define the model and review the basic points of the effective-field theory with correlations when it is applied to the present model. In section 3, the phase diagrams of the system as a function of the surface-bulk coupling are examined. Finally, we comment on our results in section 4.

II. Theoretical framework

We consider a semi-infinite simple cubic Ising ferromagnet with an antiferromagnetic surface and a modified surface-bulk coupling. Such system can be described by the following Hamiltonian:

$$H = J_S \sum_{<ij>} \sigma_i^z \sigma_j^z - J_\perp \sum_{<jk>} \sigma_j^z \sigma_k^z - J_B \sum_{<kl>} \sigma_k^z \sigma_l^z , \quad (1)$$

where σ_i^z is the z-component of spin-1/2 operator at site i. The first summation is carried out over nearest-neighbour sites located on the surface. The second summation runs over nearest-neighbour sites one located on the free surface and the other in the first layer. The third summation runs over all pairs of remaining nearest-neighbour sites. J_S and J_B denote the exchange interactions at the surface and in the bulk respectively; whereas $J_\perp$ is the coupling constant between a spin in the surface and its nearest-neighbour in the next layer.

The theoretical framework we adopt in the study of the system described by the Hamiltonian (1) is the effective-field theory based on single-site cluster theory. In this approach, attention is focused on a cluster consisting of just a single selected spin, labelled 0, and the neighbouring spins with which it directly interacts. To this end, the total Hamiltonian is split into two parts, $H = H_0 + H'$, where H_0 includes all those terms of H associated with the lattice site 0, namely

$$H_0 = -\left(\sum_j J_{0j} \sigma_j^z \right) \sigma_0^z , \quad (2)$$

$J_{0j} \equiv -J_S$ if both spins are at the surface layer, $J_{0j} \equiv J_\perp$ if one of them is located in the free surface and $J_{0j} \equiv J_B$ otherwise. The problem consists in evaluating the longitudinal site magnetisation. The starting point of our calculation is

$$\left\langle \hat{O}_0 \right\rangle = \left\langle \frac{trace_0 \left[\hat{O}_0 \exp(-\beta H_0) \right]}{trace_0 \left[\exp(-\beta H_0) \right]} \right\rangle , \quad (3)$$

Here, $trace_0$ means the partial trace with respect to the site 0, $\langle ... \rangle$ indicates the canonical thermal average and $\beta = 1/k_B T$. As we can pointed out, this relation is exact since H_0 and H' commute.

The application of (3) for the longitudinal site magnetisation of the n-th layer leads to the following expression:

$$\left\langle \sigma_{0n}^z \right\rangle = \left\langle \frac{1}{2} \tanh\left(\frac{\beta}{2} A \right) \right\rangle , \quad (4)$$

where

$$A = \sum_j J_{oj} \sigma_j^z , \quad (5)$$

Introducing the differential operator technique [20], Eq. (4) can be written as follows:

$$\left\langle \sigma_{0n}^z \right\rangle = \left\langle e^{A\nabla} \right\rangle F(x) \Big|_{x=0} , \quad (6)$$

where $\nabla = \partial / \partial x$ is a differential operator (defined as $e^{A\nabla} f(x) = f(x + A)$) and the function $F(x)$ is defined by

$$F(x) = \frac{1}{2} \tanh\left(\frac{\beta}{2} x \right) , \quad (7)$$

By assuming the statistical independence of the lattice sites, that is $\langle \sigma_i \sigma_j ... \sigma_l \rangle = \langle \sigma_i \rangle \langle \sigma_j \rangle ... \langle \sigma_l \rangle$ and using the spin-1/2 identity $\exp(\lambda \sigma_i) = \cosh(\lambda/2) + 2\sigma_i \sinh(\lambda/2)$, Eq. (6) may be written as follows:

$$\left\langle \sigma_{0n}^z \right\rangle = \prod_j \left[\cosh\left(\frac{J_{0j}}{2} \nabla \right) + 2 \left\langle \sigma_j^z \right\rangle \times \sinh\left(\frac{J_{0j}}{2} \nabla \right) \right] F(x) \Big|_{x=0} , \quad (8)$$

Denoting the ordering parameter by $\mu_n = \left\langle \sigma_{0n}^z \right\rangle$, the longitudinal magnetisation of the n-th layer is given by

$$\mu_n = \prod_{j=1}^{q} \left[a_j + 2\mu_j b_j \right] F(x) \Big|_{x=0} , \quad (9)$$

where q is the number of nearest neighbours of site 0 and the coefficients a_j and b_j are given by

$$a_S = \cosh\left(\frac{J_S}{2}\nabla\right), \quad b_S = -\sinh\left(\frac{J_S}{2}\nabla\right),$$

$$a_\perp = \cosh\left(\frac{J_\perp}{2}\nabla\right), \quad b_\perp = \sinh\left(\frac{J_\perp}{2}\nabla\right),$$

$$a_B = \cosh\left(\frac{J_B}{2}\nabla\right), \quad b_B = \sinh\left(\frac{J_B}{2}\nabla\right).$$

Eq. (9) takes the form

-for the surface ($n \equiv S$)

$$\begin{aligned}(\mu_S)_1 &= \left[a_S + 2(\mu_S)_2 b_S\right]^4 \times \\ &\quad \left[a_\perp + 2(\mu_1)_2 b_\perp\right] F(x)\big|_{x=0}, \\ (\mu_S)_2 &= \left[a_S + 2(\mu_S)_1 b_S\right]^4 \times \\ &\quad \left[a_\perp + 2(\mu_1)_1 b_\perp\right] F(x)\big|_{x=0},\end{aligned} \tag{10}$$

-for the first layer ($n = 1$)

$$\begin{aligned}(\mu_1)_1 &= \left[a_\perp + 2(\mu_S)_2 b_\perp\right] \times \\ &\quad \left[a_B + 2(\mu_1)_2 b_B\right]^4 \times \\ &\quad \left[a_B + 2(\mu_2)_2 b_B\right] F(x)\big|_{x=0}, \\ (\mu_1)_2 &= \left[a_\perp + 2(\mu_S)_1 b_\perp\right] \times \\ &\quad \left[a_B + 2(\mu_1)_1 b_B\right]^4 \times \\ &\quad \left[a_B + 2(\mu_2)_1 b_B\right] F(x)\big|_{x=0},\end{aligned} \tag{11}$$

-for any layer $n \geq 2$

$$\begin{aligned}(\mu_n)_1 &= \left[a_B + 2(\mu_{n-1})_2 b_B\right] \times \\ &\quad \left[a_B + 2(\mu_n)_2 b_B\right]^4 \times \\ &\quad \left[a_B + 2(\mu_{n+1})_2 b_B\right] F(x)\big|_{x=0}, \\ (\mu_n)_2 &= \left[a_B + 2(\mu_{n-1})_1 b_B\right] \times \\ &\quad \left[a_B + 2(\mu_n)_1 b_B\right]^4 \times \\ &\quad \left[a_B + 2(\mu_{n+1})_1 b_B\right] F(x)\big|_{x=0},\end{aligned} \tag{12}$$

Here $(\mu_n)_1$ and $(\mu_n)_2$ are the two sublattice longitudinal magnetisations of the n-th layer, respectively. Expanding the right-hand sides of (10), (11) and (12), we obtain

-for the surface ($n \equiv S$)

$$\begin{aligned}(\mu_S)_1 &= A_1(\mu_S)_2 + A_2(\mu_1)_2 + A_3(\mu_S)_2^2(\mu_1)_2 \\ &\quad + A_4(\mu_S)_2^3 + A_5(\mu_S)_2^4(\mu_1)_2, \\ (\mu_S)_2 &= A_1(\mu_S)_1 + A_2(\mu_1)_1 + A_3(\mu_S)_1^2(\mu_1)_1 \\ &\quad + A_4(\mu_S)_1^3 + A_5(\mu_S)_1^4(\mu_1)_1,\end{aligned} \tag{13}$$

-for the first layer ($n = 1$)

$$\begin{aligned}(\mu_1)_1 &= B_1(\mu_S)_2 + B_2\left(4(\mu_1)_2 + (\mu_2)_2\right) \\ &\quad + B_3(\mu_S)_2(\mu_1)_2\left(2(\mu_2)_2 + 3(\mu_1)_2\right) \\ &\quad + B_4(\mu_1)_2^2\left(2(\mu_1)_2 + 3(\mu_2)_2\right) \\ &\quad + B_5(\mu_S)_2(\mu_1)_2^3\left((\mu_1)_2 + 4(\mu_2)_2\right) \\ &\quad + B_6\left((\mu_1)_2^4(\mu_2)_2\right), \\ (\mu_1)_2 &= B_1(\mu_S)_1 + B_2\left(4(\mu_1)_1 + (\mu_2)_1\right) \\ &\quad + B_3(\mu_S)_1(\mu_1)_1\left(2(\mu_2)_1 + 3(\mu_1)_1\right) \\ &\quad + B_4(\mu_1)_1^2\left(2(\mu_1)_1 + 3(\mu_2)_1\right) \\ &\quad + B_5(\mu_S)_1(\mu_1)_1^3\left((\mu_1)_1 + 4(\mu_2)_1\right) \\ &\quad + B_6\left((\mu_1)_1^4(\mu_2)_1\right),\end{aligned} \tag{14}$$

-for any layer $n \geq 2$

$$\begin{aligned}(\mu_n)_1 &= C_1\left((\mu_{n-1})_2 + 4(\mu_n)_2 + (\mu_{n+1})_2\right) + \\ &\quad C_2(\mu_n)_2\left(2(\mu_{n-1})_2(\mu_{n+1})_2 + (\mu_n)_2 \times\right. \\ &\quad \left.\left(3(\mu_{n-1})_2 + 2(\mu_n)_2 + 3(\mu_{n+1})_2\right)\right) + \\ &\quad C_3(\mu_n)_2^3\left(4(\mu_{n-1})_2(\mu_{n+1})_2 + \right. \\ &\quad \left.(\mu_{n-1})_2(\mu_n)_2 + (\mu_n)_2(\mu_{n+1})_2\right), \\ (\mu_n)_2 &= C_1\left((\mu_{n-1})_1 + 4(\mu_n)_1 + (\mu_{n+1})_1\right) + \\ &\quad C_2(\mu_n)_1\left(2(\mu_{n-1})_1(\mu_{n+1})_1 + (\mu_n)_1 \times\right. \\ &\quad \left.\left(3(\mu_{n-1})_1 + 2(\mu_n)_1 + 3(\mu_{n+1})_1\right)\right) + \\ &\quad C_3(\mu_n)_1^3\left(4(\mu_{n-1})_1(\mu_{n+1})_1 + \right. \\ &\quad \left.(\mu_{n-1})_1(\mu_n)_1 + (\mu_n)_1(\mu_{n+1})_1\right),\end{aligned} \tag{15}$$

where the coefficients $A_i\,(i = 1-5)$, B_i $(i = 1-6)$ and C_i $(i = 1-3)$ are given in the appendix.

We note that the bulk longitudinal magnetisation μ_B is determined by setting $\mu_{n-1} = \mu_n = \mu_{n+1}$ in Eq. (15). Thus, μ_B is the solution of the equation

$$\mu_B = 6C_1\mu_B + 10C_2(\mu_B)^3 + 6C_3(\mu_B)^5. \tag{16}$$

III. Phase diagrams and discussions

In order to investigate the phase diagrams of the system described by the Hamiltonian (1), we have to solve the coupled Eqs. (13)-(15). However, we are unable to solve them analytically. Even if we use a numerical method, they must be terminated at a certain layer. Note that, as n goes to infinity, the magnetisation μ_n should approach the bulk value μ_B. For this purpose, let us assume that the magnetisations remain unaltered after the third layer, that is

$$\mu_3 = \mu_4 = ... = \mu_B,$$

which may be called the four-layer approximation.

3.1. Bulk and surface order-disorder transition temperatures

First, let us evaluate the *order-disorder transition temperatures* for the bulk and the surface ordering based on the four-layer approximation. By solving Eq. (16), the bulk critical temperature k_BT_C / J_B is determined by the equation

$$1 = 6C_1. \tag{17}$$

Comparing k_BT_C / J_B with the Monte Carlo value 1.128 [21], we remark that the obtained result 1.268 improves the mean-field value 1.500 [16].

In order to obtain the surface *order-disorder critical temperature*, we have to linearise Eqs. (13)-(15). Thus neglecting higher-order terms in the magnetisation near the critical temperature and within the four-layer approximation, we obtain

$$\begin{aligned} (\mu_S)_1 &= A_1(\mu_S)_2 + A_2(\mu_1)_2 , \\ (\mu_S)_2 &= A_1(\mu_S)_1 + A_2(\mu_1)_1 , \end{aligned} \tag{18}$$

$$\begin{aligned} (\mu_1)_1 &= B_1(\mu_S)_2 + B_2\left(4(\mu_1)_2 + (\mu_2)_2\right), \\ (\mu_1)_2 &= B_1(\mu_S)_1 + B_2\left(4(\mu_1)_1 + (\mu_2)_1\right), \end{aligned} \tag{19}$$

$$\begin{aligned} (\mu_2)_1 &= C_1\left((\mu_1)_2 + 4(\mu_2)_2 + (\mu_B)_2\right), \\ (\mu_2)_2 &= C_1\left((\mu_1)_1 + 4(\mu_2)_1 + (\mu_B)_1\right), \end{aligned} \tag{20}$$

The surface order-disorder critical temperature, when the bulk is disordered ($\mu_B = 0$), is analytically obtained through a determinantal equation. In Fig. 1, we represent the critical line of antiferromagnetic-paramagnetic surface transition (S) in the $(k_BT_C / J_B, J_S / J_B)$ plane. In all cases, when the ratio $R = J_S / J_B$ is greater than a critical value R_C, the surface may antiferromagnetically order at a temperature higher than the bulk critical temperature.

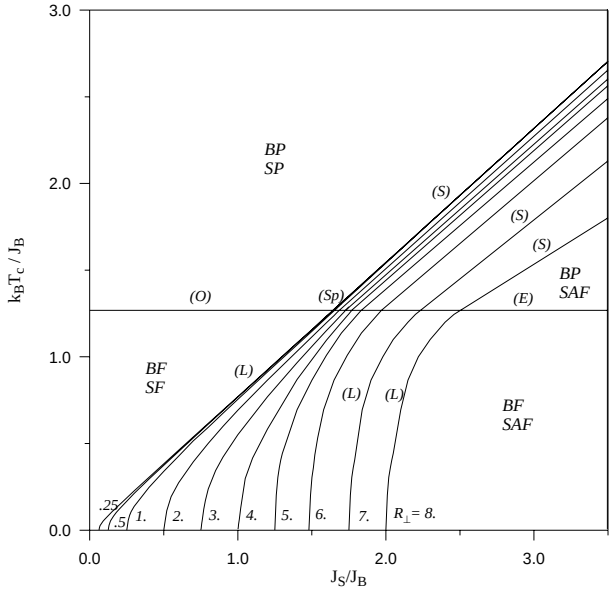

Fig. 1. Phase diagram in $T - J_S / J_B$ plane of the semi-infinite Ising model with modified surface-bulk coupling. The number accompanying each curve denotes the value of $R_\perp$

As seen from this figure, R_C depends on the value of $R_\perp = J_\perp / J_B$ and shows the influence of the surface-bulk coupling $J_\perp$ on the order-disorder surface critical temperature. Thus some surface transition lines corresponding to different values of $R_\perp$ are plotted. As clearly seen, we note that for a given value of the ratio $R = J_S / J_B$ (greater than a critical value), the surface critical temperature decreases with increasing value of $R_\perp$. From Fig. 1, we point out that the domain where the surface is antiferromagnetic (when the bulk is disordered) becomes less and less large when $R_\perp$ increases. One also notes that the critical ratio $R_C = (J_S / J_B)_C$ of the surface and bulk exchange interactions is an increasing function of $R_\perp$ as is shown in Fig. 2. We notice that, for $J_\perp$ =0, the surface becomes disconnected from the bulk and it is reduced to a two-dimensional Ising antiferromagnet. Our estimate value for the critical temperature k_BT_C / J_S is 0.772, which improves the mean-field value 1.0 (the exact value is 0.567).

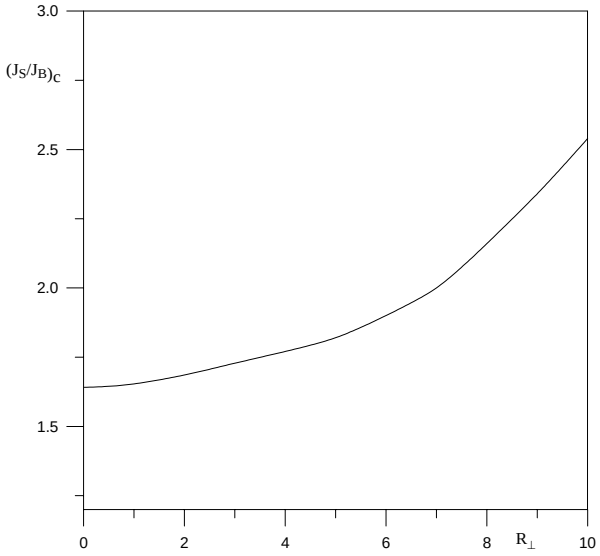

Fig. 2. Dependence of the critical ratio $R_c = (J_S / J_B)_c$ as a function $R_\perp$.

3.2. Other surface transitions

The system under investigation here undergoes other surface transitions. In fact, the steps described before do not lead to the whole phase diagram. Indeed, any two nearest neighbours on the surface interact via an antiferromagnetic coupling. At the ground state, the analysis of the Hamiltonian (1) shows that the bulk is ferromagnetic; while the surface makes a first-order transition at $R = R_\perp/4$ from anti-ferromagnetically ordered state for $R > \frac{R_\perp}{4}$ (all surface spins are anti-parallel: $(\mu_S)_1 = \pm 1, (\mu_S)_2 = \mp 1$) to

ferromagnetically ordered state for $R < \frac{R_\perp}{4}$ (all surface spins are parallel: $(\mu_S)_1 = (\mu_S)_2 = 1$). The location of this transition is obtained by equating the energies of the above phases. In order to obtain the remaining phases and transitions, we must solve numerically the coupled Eqs. (13)-(15) within the four-layer approximation scheme. The analysis of these equations leads to interesting surface phenomena. The surface behaviours, when the bulk is ordered, and their dependences on the surface-bulk coupling are also represented in Fig 1. In addition to the previous phases:

SP, BP : surface and bulk paramagnetic,

SAF, BP : surface antiferromagnetic and bulk paramagnetic,

two other phases are identified:

SF, BF : surface and bulk ferromagnetic,

SAF, BF : surface antiferromagnetic and bulk ferromagnetic.

As is seen from Fig.1, the above phases are separated by different transition lines. Among them, we find all critical lines obtained in the semi-infinite simple cubic ferromagnetic Ising model [9,15,16]. Extending the accepted terminology used in the classical semi-infinite Ising systems [22,23,24], these transitions correspond to the surface (S), the ordinary (O), the extraordinary (E) and the special (Sp) transitions. When the bulk is ferromagnetically ordered, the surface exhibits, at finite temperature, a second-order transition (L) from the ferromagnetic state (SF, BF) to the antiferromagnetic state (SAF, BF). In Fig. 1, we show the effects of the surface-bulk coupling on these transition lines. Here, we find similar phases and transitions to those obtained in the Ising system with competing surface and bulk exchange interactions $J_\perp = J_B$ done by one of us (N.B.) [25]. It is worthy of notice here that the above transition line (L) has also been found in Ising models with competing surface and bulk interactions [16,17].

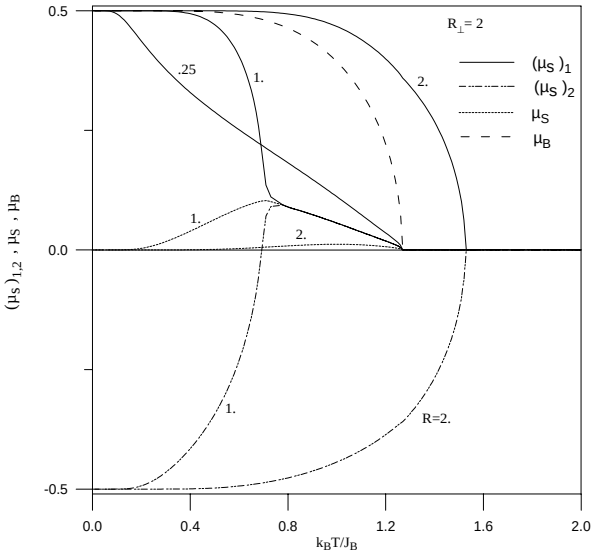

Fig. 3. Temperature dependences of $(\mu_S)_1, (\mu_S)_2$, and μ_S for the system. The number accompanying each curve denotes the value of R. The dashed line corresponds to the bulk magnetisation curve μ_B.

Indeed, the state equations (13)-(15) show interesting features of the thermal behaviours of the surface magnetisations. Fig.3 shows the temperature dependence of $(\mu_S)_1, (\mu_S)_2, \mu_S = \frac{1}{2}((\mu_S)_1 + (\mu_S)_2)$ and μ_B. They exhibit many kinds of typical behaviours depending on the value of the ratio $R = J_S / J_B$. For R greater than a ($R_\perp$-dependent) critical value R_C ($R = 2$ in Fig. 3), and at low temperature, the system is in the $BF\,SAF$ phase. With the increase of T $(\mu_S)_1, |(\mu_S)_2|$ and μ_B curves decrease and the surface sublattice magnetisations

vanish at a temperature higher than the bulk transition temperature corresponding to the transitions (S) and (E) in Fig. 1, as shown in section 3.1. For $\frac{R_\perp}{4} < R < R_C$ ($R = 1$ in Fig. 3), the surface sublattice magnetisations take their saturation values $(\mu_S)_1 = 1/2$ and $(\mu_S)_2 = -1/2$ at $T = 0\,K$ which means that the

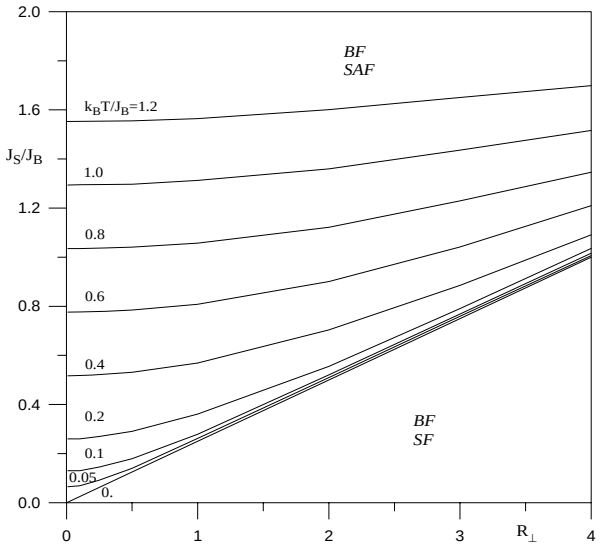

Fig. 4. Variation of the ratio of the exchange interactions $R = J_S / J_B$ as a function of $R_\perp$. The number accompanying each curve denotes the value of temperature.

surface is antiferromagnetic and the bulk is ferromagnetic $(SAF\ BF)$. We note that in this latter phase, when $T \neq 0, (\mu_S)_1$ and $(\mu_S)_2$ have both a finite total magnetisation μ_S and a finite staggered magnetisation. When the temperature is increased from zero, $(\mu_S)_1$ and $|(\mu_S)_2|$ decrease as long as the system is still in $SAF\ BF$ phase. Then, at a critical temperature, the sublattice magnetisation $(\mu_S)_2$ changes its sign, undergoing a second order transition (L) (see Fig. 1) from the $SAF\ BF$ phase to $SF\ BF$ phase. In this case the total surface magnetisation μ_S passes through a maximum, then decreases and vanishes at the bulk transition temperature. This latter transition corresponds to the ordinary transition (O) in Fig. 1. Finally, when $R < \frac{R_\perp}{4}$ ($R = 0.25$ in Fig. 3), the bulk promotes its order to the surface in such a way that the bulk and the surface are both paramagnetic or ferromagnetic. Thus, the surface and bulk magnetisations take their saturation values at $T = 0\,K$ and vanish at the bulk transition temperature. This transition corresponds to the ordinary transition denoted (O) in Fig. 1. On the other hand and as we can point out from Fig. 1, the location of the transition line (L) depends qualitatively and quantitatively on the strength of $R_\perp$, specially at very low temperatures. In order to clarify this situation, we plot in Fig. 4 the phase diagram in $R_\perp - R$ plane at different temperatures (below $k_B T_C / J_B$). As clearly seen in this figure, we note that, at very low temperature, the ratio R at which the surface undergoes (L) transition, is very sensitive to the ratio $R_\perp$; but this latter has not a significant effect on that transition when the temperature approaches its bulk critical value.

IV. Conclusions

In this paper, we have investigated the surface phase diagrams of the semi-infinite simple-cubic spin-1/2 Ising ferromagnet with an antiferromagnetic interaction $(-J_S < 0)$ on the surface and a modified surface-bulk coupling $J_\perp$. To do this, we have used an effective-field method within the framework of a single-site cluster theory. In this approach, we have derived the state equations using the differential operator technique and neglecting correlations between different sites. Using these coupled equations within the four-layer approximation, rich phase diagram have been discovered and some significant results have been obtained.

Let us summarise by stating the main results of this investigation. We identified four physically different phases separated by five transition lines. In particular, when the bulk is disordered, if the ratio $R = J_S / J_B$ is greater than a ($R_\perp = J_\perp / J_B$ -dependent) critical value R_C, the surface may antiferromagnetically order at a temperature (surface transition) higher than the bulk. On the other hand, when the bulk is ferromagnetically ordered, the surface may undergo, at finite temperature, a second-order phase transition (L) from the ferromagnetic order to the antiferromagnetic one. Its location in the phase diagram depends on the strength of the surface-bulk coupling $J_\perp$.

Appendix

The coefficients A_i ($i = 1-5$), B_i ($i = 1-6$) and C_i ($i = 1-3$) in Eqs. (13)-(20) are defined by

$$A_1 = 8a_S^3 b_S a_\perp F(x)\big|_{x=0},$$
$$A_2 = 2a_S^4 b_\perp F(x)\big|_{x=0},$$
$$A_3 = 48a_S^2 b_S^2 b_\perp F(x)\big|_{x=0},$$
$$A_4 = 32a_S b_S^3 a_\perp F(x)\big|_{x=0},$$
$$A_5 = 32b_S^4 b_\perp F(x)\big|_{x=0},$$
$$B_1 = 2a_B^5 b_\perp F(x)\big|_{x=0},$$
$$B_2 = 2a_\perp a_B^4 b_B F(x)\big|_{x=0},$$
$$B_3 = 16a_B^3 b_\perp b_B^2 F(x)\big|_{x=0},$$
$$B_4 = 16a_\perp a_B^2 b_B^3 F(x)\big|_{x=0},$$
$$B_5 = 32a_B b_\perp b_B^4 F(x)\big|_{x=0},$$
$$B_6 = 32a_\perp b_B^5 F(x)\big|_{x=0},$$
$$C_1 = 2a_B^5 b_B F(x)\big|_{x=0},$$
$$C_2 = 16a_B^3 b_B^3 F(x)\big|_{x=0},$$
$$C_3 = 32\,a_B b_B^5 F(x)\big|_{x=0}.$$

[1] K. Binder, in: C. Domb, J. L. Lebowitz (Eds.), Phase Transitions and Critical Phenomena, Vol. 8, Academic Press, New York, 1983.
[2] H. W. Diehl, in: C. Domb, J. L. Lebowitz (Eds.), Phase Transitions and Critical Phenomena, Vol. 10, Academic Press, New York, 1986.
[3] T. Kaneyoshi, Introduction to Surface Magnetism, CRC Press, Boca Raton, FL, USA, 1991.
[4] D. L. Mills, Phys. Rev. B 3 (1971) 3887.
[5] T. C. Lubensky, M. H. Rubin, Phys. Rev. B 12 (1975) 3885; B 11 (1975) 4533.
[6] J. M. Sanchez, J. L. Moran-Lopez, in: L. M. Flicov, J. L. Moran-Lopez (Eds.), Magnetic Properties of Low Dimensional Systems, Springer, Berlin, 1986.
J. L. Moran-Lopez, J. M. Sanchez, Phys. Rev. B 39 (1989) 9746.
[7] T. Kaneyoshi, I. Tamura, E. F. Sarmento, Phys. Rev. B 28 (1983) 6491.
[8] A. Benyoussef, A. El Kenz, phys. stat. sol. (b) 165 (1991) K23.
[9] A. Benyoussef, N. Boccara, M. Saber, J. Phys. C 18 (1985) 4275.
[10] T. W. Burkhardt, E. Eisenrigler, Phys. Rev. B 16 (1977) 3213.
[11] N. M. Svrakic, M. Wortis, Phys. Rev. B 15 (1977) 395.
[12] O. Nagai, M. Toyonaga, J. Phys. C 14 (1981) L545.
[13] C. Tsallis, E. F. Sarmento, J. Phys. C 18 (1985) 2777.
[14] K. Binder, D. P. Landau, Phys. Rev. Lett. 52 (1984) 318.
[15] D. P. Landau, K. Binder, Phys. Rev. B 41 (1990) 4633.
[16] K. Binder, P. C. Hohenberg, Phys. Rev. B. 9 (1974) 2194.
[17] E. F. Sarmento, C. Tsallis, J. Phys. C 47 (1986) 1115.
[18] K. Binder, D. P. Landau, Surf. Sci. 151 (1985) 409.
[19] F. Zhang, S. Thevuthasan, R. T. Scalettar, R. R. P. Singh, C. S. Fadley, Phys. Rev. B 51 (1995) 12468.
[20] R. Honmura, T. Kaneyoshi, J. Phys. C 12 (1979) 3979.
[21] A. J. Liu, M. E. Fisher, Physica A 156 (1989) 35.
[22] A. Dakhama, A. Fathi, N. Benayad, Eur. Phys. J. B 21 (2001) 393.
[23] N. Benayad, J. Zittartz, Z. Phys. B Condens Matter 81 (1990) 107.
[24] A. J. Bray, M. A. Moore, J. Phys. A 10 (1977) 1927.
[25] L. Khaya, N. Benayad, A. Dakhama, phys. stat. sol. (b) 241 (2004) 1078.